International Journal of Fatigue 83 (2016) 59–65

Contents lists available at ScienceDirect

International Journal of Fatigue

journal homepage: www.elsevier.com/locate/ijfatigue

Corrosion fatigue assessment of creep-resistant magnesium alloy Mg–4Al–2Ba–2Ca in aqueous sodium chloride solution

Philipp Wittke [a,*], Martin Klein [a], Hajo Dieringa [b], Frank Walther [a]

[a] TU Dortmund University, Materials Test Engineering (WPT), Baroper Str. 303, D-44227 Dortmund, Germany
[b] Helmholtz-Zentrum Geesthacht (HZG), Magnesium Innovations Centre (MagIC), Max-Planck-Str. 1, D-21502 Geesthacht, Germany

ARTICLE INFO

Article history:
Received 4 November 2014
Received in revised form 18 March 2015
Accepted 2 April 2015
Available online 9 April 2015

Dedicated to Prof. Dr.-Ing. Dietmar Eifler (Technical University of Kaiserslautern) on the occasion of his 65th birthday.

Keywords:
Magnesium alloy
Mg–4Al–2Ba–2Ca
Corrosion fatigue
Potentiodynamic polarization
Immersion

ABSTRACT

Low corrosion resistance of magnesium alloys strongly limits their application range. This study aims at the investigation of corrosion influence on microstructure and depending mechanical properties of newly developed magnesium alloy Mg–4Al–2Ba–2Ca. The fatigue properties of this creep-resistant magnesium alloy were investigated under three corrosive environments: double distilled water, 0.01 and 0.1 mol L^{-1} NaCl solutions. Potentiodynamic polarization measurements and immersion tests were performed to estimate the corrosion behaviour. Specimen surfaces were observed using light and scanning electron microscopy for microstructure-related assessment of corrosion mechanisms. The corrosion fatigue behaviour was characterized in continuous load increase tests using plastic strain and electrochemical measurements. Continuous load increase tests allow estimating the fatigue limit and determining the failure stress amplitude with one single specimen. Fatigue results showed a significant decrease in the estimated fatigue limit and determined failure stress amplitude with increasing corrosion impact of the environments. This corrosion–structure–property relation was quantitatively described by means of model-based correlation approaches and failure hypotheses. Plastic strain amplitude and deformation-induced changes in electrochemical measurands can be equivalently applied for precise corrosion fatigue assessment.

1. Introduction

Due to their low density, beneficial strength to weight ratio and good castability, magnesium alloys are very attractive for light weight applications [1]. However, the application range of magnesium alloys is strongly limited due to their low corrosion resistance, especially in electrolytes containing chlorides [2]. The low corrosion resistance also impairs the fatigue properties. The aim of this study was the investigation of the influence of corrosion on the microstructure and the dependent mechanical properties under cyclic load for the newly developed creep-resistant magnesium alloy Mg–4Al–2Ba–2Ca. The main focus was the evaluation of the corrosion fatigue damage. Microstructure-related deformation behaviour and underlying deformation mechanisms as well as the remaining fatigue life were investigated in dependence of defined corrosion stages.

2. Material

The chemical composition of the investigated Mg–4Al–2Ba–2Ca alloy for the outer area of the cast (d = 105 mm), measured by an energy dispersive X-ray fluorescence spectrometer (Shimadzu, EDX 720P), is given in Table 1. The outer area represents the outer 45% cross-sectional area of the cylindrical cast.

The alloy was mixed from a melt containing very pure magnesium (>99.9%), aluminium (>99.9%), barium (>99.0%), and calcium (99.5%). The temperature of the melt was kept constant and it was stirred at 720 °C for ten minutes. Mg–4Al–2Ba–2Ca was cast using a permanent mould, direct chill casting process. After melting the alloy and keeping it at 720 °C, the melt was poured into preheated cylindrical moulds, which were placed into a round three-zone resistance furnace. A constant flux of Ar-SF6 (5:1) cover gas was introduced on top of the melt during the complete casting. The steel mould containing Mg–4Al–2Ba–2Ca melt was lowered into a water bath located beneath the ring furnace (Fig. 1). Since the mould descended at a constant speed into the water bath, the solidification started at the bottom of the mould. This process results in a very dense casting, because the remaining melt is always above the solidified material, which leads to shrinkage

* Corresponding author. Tel.: +49 231 755 8031; fax: +49 231 755 8029.
E-mail address: philipp.wittke@tu-dortmund.de (P. Wittke).

http://dx.doi.org/10.1016/j.ijfatigue.2015.04.001
0142-1123/

Table 1
Chemical composition (wt%) of Mg–4Al–2Ba–2Ca alloy for the outer area of the cast.

Element	Al	Ba	Ca	Fe	Mg
Mg–4Al–2Ba–2Ca	5.7	1.7	1.6	0.02	Bal.

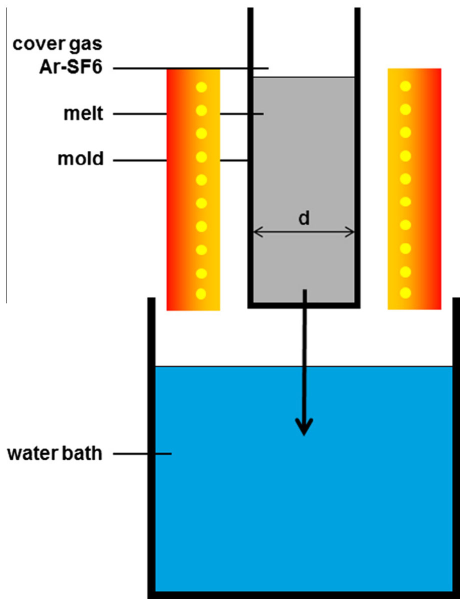

Fig. 1. Sketch of permanent mould direct chill casting process.

feeding at every point. The casts exhibit low porosity without cracks or inclusions and homogenous distributed alloying elements without macrosegregation, as reported for optimized permanent mold casting of the magnesium alloy Mg–9Al–10Gd by Elsayed et al. [3].

Specimens for tensile and fatigue tests were prepared from the outer area of the cast. The specimen geometry is given in Fig. 2.

SEM micrographs (Fig. 3) and EDX analyses indicate the texture to consist of three phases. At the grain boundaries of the primary α-Mg phase a compact Ba-rich phase ($Mg_{21}Al_3Ba_2$) and a lamellar Ca-rich phase (Al_2Ca) precipitate [4]. Area fractions of the phases were determined by means of digital image analysis methods (PixelFerber, phase-fraction software) over thresholding in grayscale intensity images (Table 2). The area fractions of the inner area of the cast differed insignificantly from the outer area.

Micro-hardness tests showed a local dependence in contrast to the microscopic structure investigations. At the outer area of the cast the micro-hardness of the $Mg_{21}Al_3Ba_2$ phase (222 HV0.005) was lower than in the middle area (353 HV0.005), whereas the micro-hardness of the Al_2Ca phase (116 HV0.005) was higher than in the middle area (78 HV0.005). The α-Mg phase has the same micro-hardness in the outer and middle area of the cast (67

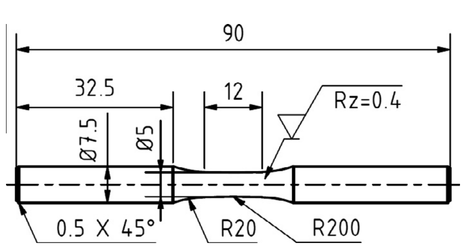

Fig. 2. Specimen geometry for mechanical investigations (all dimensions in mm).

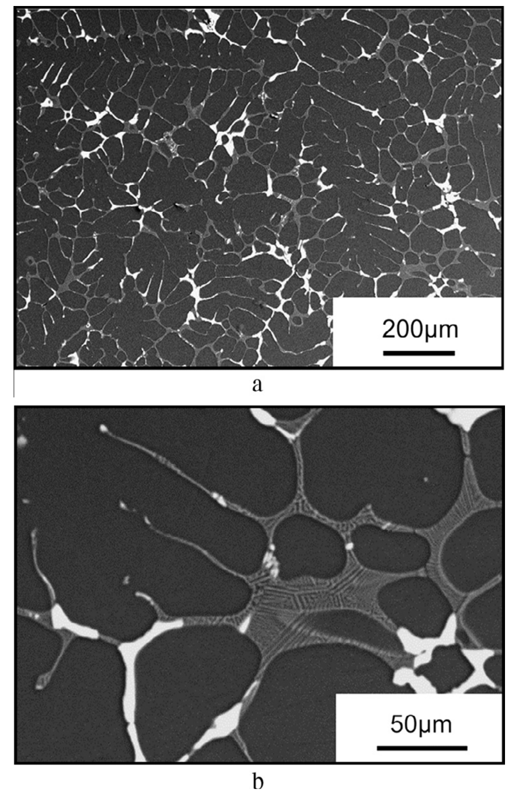

Fig. 3. SEM images of Mg–4Al–2Ba–2Ca in initial state; (a) overview and (b) detail.

Table 2
Mechanical properties, hardness and area fractions for the outer area of the cast.

	Mg–4Al–2Ba–2Ca
Yield strength $R_{p0.01}$ (MPa)	15
Tensile strength R_m (MPa)	122
Fracture strain (%)	1.72
Vickers macro-hardness (HV10)	53
Vickers micro-hardness $Mg_{21}Al_3Ba_2$ phase (HV0.005)	222
Vickers micro-hardness Al_2Ca phase (HV0.005)	116
Area fraction $Mg_{21}Al_3Ba_2$ phase (area%)	5.0
Area fraction Al_2Ca phase (area%)	10.8

HV0.005). The local dependence of the micro-hardness is compensated by the integral determination of the macro-hardness, which is almost constant over the cross-section (53 ± 2 HV10), as already described in a previous paper [5].

For the corrosion and fatigue investigations only specimens from the outer area of the cast were used to ensure a comparability of the results.

In Table 2 the results from tensile tests, Vickers hardness and area fractions for the outer area of the cast are summarized.

3. Experimental setup

The corrosion behaviour was investigated using potentiodynamic polarization measurements and immersion tests in double distilled water (i.e. 0 mol L^{-1} NaCl solution), 0.01 and 0.1 mol L^{-1} NaCl solution at pH7, in which the pH values were adjusted using a 0.1 M KOH solution. For the potentiodynamic polarization measurements, a standard three electrode system was used with a saturated calomel electrode (SCE) as reference electrode, a graphite electrode as counter electrode and a Mg–4Al–2Ba–2Ca specimen as working electrode (Fig. 4a). Before